

Diffusion of surface gravity wave action by mesoscale turbulence at the sea surface

Journal:	<i>Journal of Fluid Mechanics</i>
Manuscript ID	JFM-19-RP-1880
mss type:	JFM Rapids
Date Submitted by the Author:	06-Dec-2019
Complete List of Authors:	Villas Bôas, Ana Beatriz; University of California San Diego, Scripps Institution of Oceanography Young, William; University of California, San Diego, Scripps Institution of Oceanography
Keyword:	Waves in random media < Acoustics, Air/sea interactions < Geophysical and Geological Flows, Surface gravity waves < Waves/Free-surface Flows

SCHOLARONE™
Manuscripts

Diffusion of surface gravity wave action by mesoscale turbulence at the sea surface

Ana B. Villas Bôas ^{1†} and William R. Young¹

¹Scripps Institution of Oceanography, La Jolla, CA, USA

(Received xx; revised xx; accepted xx)

We use a multiple-scale expansion approach to average the wave action balance equation over an ensemble of sea-surface velocity fields characteristic of the ocean mesoscale and submesoscale. Assuming that the statistical properties of the flow are stationary and homogeneous, we derive an expression for a diffusivity tensor of surface wave action density. The small parameter in this multiple-scale expansion is the ratio of surface current speed to gravity wave group speed. For isotropic currents, the action diffusivity is expressed in terms of the kinetic energy spectrum of the flow. A Helmholtz decomposition of the sea-surface currents into solenoidal (vortical) and potential (divergent) components shows that, to leading order, the potential component of the surface velocity field has no effect on the diffusivity of wave action: only the vortical component of the sea-surface velocity results in diffusion of surface wave action. We validate our analytic results for the action diffusivity by Monte Carlo ray-tracing simulations through an ensemble of stochastic velocity fields.

Key words:

1. Introduction

Surface gravity waves are an important route by which the ocean exchanges energy, momentum, heat, and gases with the overlying atmosphere (Cavaleri *et al.* 2012; Villas Bôas *et al.* 2019). Sea-surface currents modify the wavenumber, direction, and amplitude of surface waves, and affect the spatial variability of the wave field. The effect of currents on waves under the WKB approximation has been well studied (Kenyon 1971; Peregrine 1976; White & Fornberg 1998; Heller *et al.* 2008; Gallet & Young 2014; Henderson *et al.* 2006). But the sparseness of ocean current observations makes it difficult to explicitly account for wave-current interactions in numerical surface wave models. Thus, instead of explicit resolving sea-surface currents, a statistical approach to the effect of currents on surface waves is required.

Recent studies of surface wave-current interactions (e.g., Ardhuin *et al.* 2017; Quilfen *et al.* 2018; Quilfen & Chapron 2019) show that the sea-state variability at meso- and submesoscales (1-150 km) is dominated by the variability of the current field. At these scales, horizontally divergent motions associated with tides, inertia-gravity waves, and fronts contribute significantly to the surface kinetic energy (Bühler *et al.* 2014; Rocha *et al.* 2016; D’Asaro *et al.* 2018). If surface gravity waves respond differently to divergent than to rotational flows — and we show here that they do — then changes in the dominant regime of surface currents can result in significant changes in the surface-wave field. This

† Email address for correspondence: avillasboas@ucsd.edu

offers the possibility that observations of surface gravity waves might be used to probe the structure of submesoscale ocean turbulence.

In the context of internal gravity waves, McComas & Bretherton (1977) showed how scale-separated wave interactions can be analyzed with the WKB approximation and understood as diffusion of wave action. The induced-diffusion approximation of McComas & Bretherton has recently been developed and extended by Kafiabad, Savva & Vanneste (2019, KSV, hereafter) to obtain an action-diffusion equation for the scattering of internal gravity waves by mesoscale ocean turbulence. In section 2 and in appendix A we use the formalism of KSV to derive an expression for a diffusivity tensor of surface wave action; we show that the horizontally divergent component of the sea-surface velocity has no effect on action diffusivity. In section 3 we consider the simplifications that result from assuming that the sea-surface velocity has isotropic statistics. In section 4 the analytic results are tested with Monte Carlo ray-tracing through an ensemble of stochastic velocity fields.

2. The induced diffusion approximation

For linear deep-water surface waves, the Doppler-shifted dispersion relation is

$$\omega(t, \mathbf{x}, \mathbf{k}) = \sigma + \mathbf{k} \cdot \mathbf{U}(t, \mathbf{x}), \quad (2.1)$$

where $\mathbf{k} = (k_1, k_2)$ is the wavenumber, $\sigma = \sqrt{gk}$ is the intrinsic wave frequency, with $k = |\mathbf{k}|$ and g the gravitational acceleration. Also in (2.1), $\mathbf{U}(t, \mathbf{x}) = (U_1, U_2)$ is the horizontal current at the sea-surface. Provided that $\mathbf{U}(t, \mathbf{x})$ is slowly varying with respect to the waves, i.e., the temporal scales of variations in the current field are longer and the spatial scales are larger than those of the waves, wave kinematics is described by the ray equations. Using index notation the ray equations are

$$\dot{x}_n = \partial_{k_n} \omega = c_n + U_n, \quad \text{and} \quad \dot{k}_n = -\partial_{x_n} \omega = -U_{m,n} k_m, \quad (2.2)$$

where $c_n = \partial_{k_n} \sigma(k)$ is the group velocity. Under the same assumptions, wave dynamics is governed by the conservation of wave-action density $A(\mathbf{x}, \mathbf{k}, t)$

$$\partial_t A + \dot{x}_n \partial_{x_n} A + \dot{k}_n \partial_{k_n} A = 0, \quad (2.3)$$

with \dot{x}_n and \dot{k}_n given by (2.2) (Phillips 1966; Mei 1989).

We follow KSV and develop a multiple-scale solution that enables one to average (2.3) over the ensemble of velocity fields \mathbf{U} (see appendix A). Assuming that the statistical properties of \mathbf{U} are stationary and homogeneous, one finds that

$$\partial_t \bar{A} + c_n \partial_{x_n} \bar{A} = \partial_{k_j} D_{jn} \partial_{k_n} \bar{A}, \quad (2.4)$$

where \bar{A} denotes the ensemble average of A . The diffusivity tensor D_{jn} in (2.4) is expressed in terms of the two-point velocity correlation tensor

$$V_{im}(\mathbf{x} - \mathbf{x}') \stackrel{\text{def}}{=} \langle U_i(\mathbf{x}) U_m(\mathbf{x}') \rangle. \quad (2.5)$$

Because of the assumption of spatial homogeneity, V_{im} depends only on the separation $\mathbf{r} = \mathbf{x} - \mathbf{x}'$ of the two points. The most convenient formula for explicit calculation of D_{jn} is the Fourier space result

$$D_{jn} = \frac{k_j k_m k}{4\pi c} \int q_j q_n \tilde{V}_{im}(\mathbf{q}) \delta(\mathbf{q} \cdot \mathbf{k}) d\mathbf{q}, \quad (2.6)$$

where $c = g/2\sigma$ is the magnitude of the group velocity and

$$\tilde{V}_{im}(\mathbf{q}) = \int e^{-i\mathbf{r}\cdot\mathbf{q}} V_{im}(\mathbf{r}) d\mathbf{r} \quad (2.7)$$

is the Fourier transform of $V_{im}(\mathbf{r})$. (In (2.6) and (2.7) the integrals cover the entire two-dimensional planes (q_1, q_2) and (r_1, r_2) respectively.) The diffusivity in (2.6) is the two-dimensional equivalent of (A7) in KSV. Our appendix A derivation, however, assumes only spatial homogeneity and stationarity of the velocity \mathbf{U} , and does not require incompressibility of \mathbf{U} .

One can verify from (2.6) that $D_{jn}k_n = 0$ and therefore there is no diffusion of wave action in the radial direction in \mathbf{k} -space. Fast surface-wave packets propagate through a frozen field of mesoscale eddies and thus preserve the absolute frequency $\sqrt{gk} + \mathbf{U} \cdot \mathbf{k}$. But with $\epsilon \ll 1$ (appendix A) the Doppler shift $\mathbf{U} \cdot \mathbf{k}$ is small relative to \sqrt{gk} and so, at the order of (2.6), the wavenumber k is constant. Thus absolute frequency conservation underlies the absence of radial \mathbf{k} -diffusion.

3. Diffusion of wave action density by isotropic velocity fields

The derivation of (2.6) makes essential use of the assumption that the spatial statistics of \mathbf{U} are spatially homogeneous. We now make the further assumption that the statistical properties of \mathbf{U} are also isotropic and investigate the contributions of vertical vorticity and horizontal divergence to D_{jn} . We follow Bühler *et al.* (2014) and represent the velocity field with a 2D Helmholtz decomposition into rotational (solenoidal) and irrotational (potential) components

$$(\mathbf{U}, V) = (\phi_x - \psi_y, \phi_y + \psi_x). \quad (3.1)$$

The streamfunction ψ and velocity potential ϕ have the two-point correlation functions

$$C^\psi(r) = \langle \psi(\mathbf{x})\psi(\mathbf{x}') \rangle, \quad \text{and} \quad C^\phi(r) = \langle \phi(\mathbf{x})\phi(\mathbf{x}') \rangle. \quad (3.2)$$

If the velocity ensemble is not mirror invariant under reflexion with respect to an axis in the (x, y) -plane, then there might also be a “cross-correlation” between ψ and ϕ

$$C^{\psi\phi}(r) \stackrel{\text{def}}{=} \langle \psi(\mathbf{x})\phi(\mathbf{x}') \rangle = \langle \psi(\mathbf{x}')\phi(\mathbf{x}) \rangle. \quad (3.3)$$

Because of isotropy, the scalar correlation functions introduced in (3.2) and (3.3) depend only on the distance $r = |\mathbf{r}|$ between points \mathbf{x} and \mathbf{x}' . Therefore, $\partial_{r_i} = \partial_{x_i} = -\partial_{x'_i}$. Using the notation $\mathbf{r} = (r_1, r_2)$, the V_{11} component of the velocity autocorrelation tensor in (2.5) can be expressed in terms of the scalar correlation functions as

$$V_{11}(\mathbf{r}) = \langle U(\mathbf{x})U(\mathbf{x}') \rangle, \quad (3.4)$$

$$= \langle \psi_y \psi_{y'} \rangle - \langle \psi_{y'} \phi_x \rangle - \langle \psi_y \phi_{x'} \rangle + \langle \phi_x \phi_{x'} \rangle, \quad (3.5)$$

$$= -\partial_{r_2}^2 C^\psi + 2\partial_{r_1} \partial_{r_2} C^{\psi\phi} - \partial_{r_1}^2 C^\phi. \quad (3.6)$$

Similar calculations for the other components of V_{im} result in

$$V_{im} = V_{im}^\psi + V_{im}^{\psi\phi} + V_{im}^\phi, \quad (3.7)$$

with

$$V_{im}^\psi = \begin{bmatrix} -\partial_{r_2}^2 & \partial_{r_1} \partial_{r_2} \\ \partial_{r_1} \partial_{r_2} & -\partial_{r_1}^2 \end{bmatrix} C^\psi, \quad V_{im}^\phi = - \begin{bmatrix} \partial_{r_1}^2 & \partial_{r_1} \partial_{r_2} \\ \partial_{r_1} \partial_{r_2} & \partial_{r_2}^2 \end{bmatrix} C^\phi, \quad (3.8)$$

$$\text{and} \quad V_{im}^{\psi\phi} = \begin{bmatrix} 2\partial_{r_1} \partial_{r_2} & \partial_{r_2}^2 - \partial_{r_1}^2 \\ \partial_{r_2}^2 - \partial_{r_1}^2 & 2\partial_{r_1} \partial_{r_2} \end{bmatrix} C^{\psi\phi}. \quad (3.9)$$

The Fourier transform of (3.8) and (3.9) follows with $\partial_{r_i} \mapsto iq_i$ and is equal to

$$\tilde{V}_{im}^{\psi}(\mathbf{q}) = (q^2 \delta_{im} - q_i q_m) \tilde{C}^{\psi}(q), \quad \tilde{V}_{im}^{\phi}(\mathbf{r}) = q_i q_m \tilde{C}^{\phi}(q), \quad (3.10)$$

$$\text{and} \quad \tilde{V}_{im}^{\psi\phi}(\mathbf{q}) = (q_i q_m^{\perp} + q_i^{\perp} q_m) \tilde{C}^{\psi\phi}(q), \quad (3.11)$$

where $\mathbf{q}^{\perp} = (-q_2, q_1)$ is the perpendicular vector to $\mathbf{q} = (q_1, q_2)$. Also in (3.10) and (3.11)

$$\tilde{C}^{\psi}(q) = 2\pi \int_0^{\infty} C^{\psi}(r) J_0(qr) r dr, \quad (3.12)$$

with J_0 the Bessel function of order zero, is the Fourier transform of the axisymmetric function $C^{\psi}(r)$. The expressions for $\tilde{C}^{\phi}(q)$ and $\tilde{C}^{\psi\phi}(q)$ are analogous to (3.12).

Substituting (3.10) and (3.11) into (2.6) we have

$$k_i k_m \tilde{V}_{im}(\mathbf{q}) = k^2 q^2 \tilde{C}^{\psi}(q) + \dots \quad (3.13)$$

where \dots above indicates the three other terms that arise from contracting (3.10) and (3.11) with $k_i k_m$. Each of these three terms, however, contains a factor $\mathbf{k} \cdot \mathbf{q}$. Courtesy of $\delta(\mathbf{k} \cdot \mathbf{q})$ in the integrand of (2.6), the \dots in (3.13) makes no contribution to D_{jn} and the diffusivity tensor reduces to

$$D_{jn}(\mathbf{k}) = \frac{k^3}{4\pi c} \int q^2 q_j q_n \tilde{C}^{\psi}(q) \delta(\mathbf{q} \cdot \mathbf{k}) d\mathbf{q}, \quad (3.14)$$

where the integral covers the entire (q_1, q_2) -plane. The diffusion tensor in (3.14) does not depend on the velocity potential ϕ . Using $\delta(\mathbf{q} \cdot \mathbf{k})$ to evaluate one of the two integrals in (3.14) one obtains

$$D_{jn}(\mathbf{k}) = \frac{1}{2\pi c} \begin{bmatrix} k_2^2 & -k_1 k_2 \\ -k_1 k_2 & k_1^2 \end{bmatrix} \int_0^{\infty} q^4 \tilde{C}^{\psi}(q) dq. \quad (3.15)$$

It is remarkable that the compressible and irrotational component of the velocity field, produced by the velocity potential ϕ , makes no contribution to the action diffusion tensor in (3.15). Dysthe (2001) shows that in the weak-current limit (that is $\epsilon \ll 1$ in appendix A) the ray curvature is equal to ζ/c where $\zeta = \psi_{xx} + \psi_{yy}$ is the vertical vorticity of the surface currents; see section 68 of Landau & Lifshitz (1987) and Gallet & Young (2014) for alternative derivations. These ray-tracing results rationalize the result in (3.15) that diffusion of surface-wave action by sea-surface currents is produced only by the vortical component of the sea-surface velocity.

This effect is illustrated in figure 1, where we show ray trajectories obtained from numerically solving the ray equations (2.2) for waves with period of 10s propagating through three different types of surface flows (purely solenoidal, purely potential, and combined solenoidal and potential). These synthetic surface currents were created from a scalar function with random phase and prescribed spectral slope ($q^{-2.5}$ in this case). In panel A this function is used as a streamfunction ψ to generate an incompressible vortical flow. In panel B the same function is used as a velocity potential ϕ to generate an irrotational horizontally divergent flow. In panels B and E, with pure potential flow, the ray trajectories are close to straight lines i.e., there is almost no scattering. The flow in panel C is constructed by summing the velocity fields in A and B. Even though the flow in C is twice as energetic as that in A, the ray trajectories in D and F are very similar. This is a striking confirmation of (3.14): the diffusivity is not affected by ϕ .

Because $D_{jn} k_n = 0$, the diffusive flux of wave action, $-D_{jn} \partial_{k_n} \bar{A}$, is in the direction of $\mathbf{k}^{\perp} = k \hat{\theta}$ where (k, θ) are polar coordinates in the \mathbf{k} -plane and $\hat{\theta}$ is a unit vector in the θ -direction. Using these polar coordinates simplifies the ∂_{k_j} and ∂_{k_n} derivatives on the

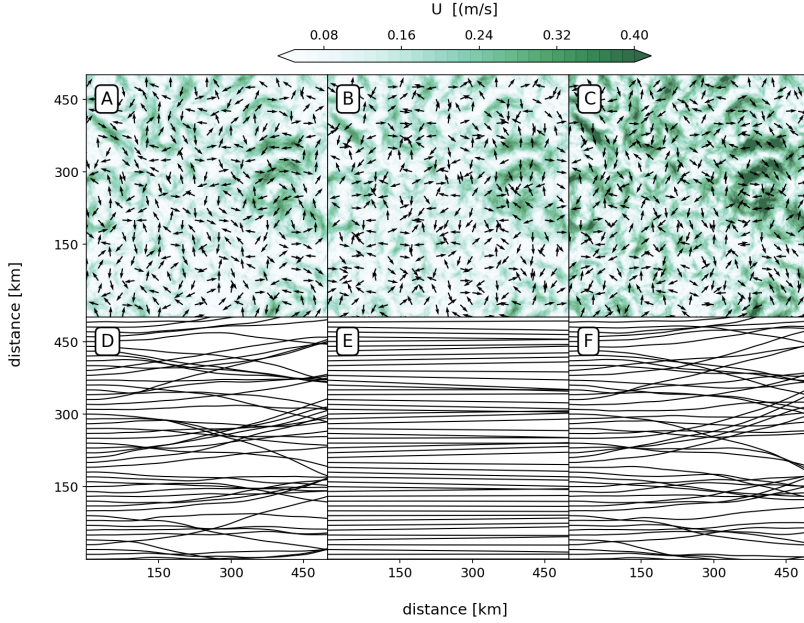


FIGURE 1. Illustration of the effects of different surface flow regimes on the diffusion of surface waves. Surface flow fields are shown on the top row and the respective ray trajectories in the bottom row. Panels A and D show solenoidal flow; panels B and E potential flow. Panels C and F show a combination of solenoidal and potential flows (the velocity in panel C is the sum of the velocities in panels A and B). The mean kinetic energy of A and B are equal, whereas panel C has twice that of A and B. All rays are initialized from the left side of the domain at $x = 0$ with direction $\theta = 0^\circ$ and period equal to 10s.

right of (2.4) so that the averaged action equation becomes

$$\bar{A}_t + c \cos \theta \bar{A}_x + c \sin \theta \bar{A}_y = \alpha \bar{A}_{\theta\theta}, \quad (3.16)$$

where

$$\alpha(k) = \frac{1}{2\pi c} \int_0^\infty q^4 \tilde{C}^\psi(q) dq. \quad (3.17)$$

To conclude this section we express α in (3.17) in terms of the energy spectrum of the solenoidal component of the velocity $\tilde{E}^\psi(q)$, related to $\tilde{C}^\psi(q)$ by

$$\tilde{E}^\psi(q) = \frac{q^3}{4\pi} \tilde{C}^\psi(q). \quad (3.18)$$

The spectrum is normalized so that the root-mean-square velocity of the solenoidal component, \mathcal{U}_ψ , is

$$\mathcal{U}_\psi^2 = \langle \psi_x^2 \rangle = \langle \psi_y^2 \rangle = \frac{1}{2} \langle |\nabla \psi|^2 \rangle = \int_0^\infty \tilde{E}^\psi(q) dq. \quad (3.19)$$

Then $\alpha(k)$ can be written as

$$\alpha(k) = \frac{2}{c} \int_0^\infty q \tilde{E}^\psi(q) dq. \quad (3.20)$$

The total energy spectrum is $\tilde{E}^\psi(q) + \tilde{E}^\phi(q)$, where $\tilde{E}^\phi(q)$ is obtained by $\psi \mapsto \phi$ in (3.19). But as anticipated in figure 1, the diffusivity $\alpha(k)$ in (3.20) depends only on the spectrum of the solenoidal component, $\tilde{E}^\psi(q)$.

4. A numerical example using ray tracing

Equation (3.16) has an exact solution that can be used to test (3.20). Begin by noting that

$$\frac{d}{dt} \iiint A \, dx dy d\theta = 0, \quad (4.1)$$

where the integrals above are over the whole (x, y) -plane and over $-\pi < \theta \leq \pi$. This is, of course, conservation of action. Multiplying (3.16) by $\cos \theta$ and integrating over (x, y, θ) one obtains

$$\frac{d}{dt} \iiint \cos \theta \, A \, dx dy d\theta = -\alpha \iiint \cos \theta \, A \, dx dy d\theta. \quad (4.2)$$

Combining the time integrals of (4.1) and (4.2) we find

$$\langle \cos \theta \rangle = \langle \cos \theta \rangle_0 e^{-\alpha t}, \quad (4.3)$$

where $\langle \rangle$ denotes the action-weighted average and $\langle \cos \theta \rangle_0$ is the initial value of $\langle \cos \theta \rangle$. At large times $\langle \cos \theta \rangle \rightarrow 0$ with an e -folding time α^{-1} : this is long-time isotropization of the wave field by eddy scattering. To investigate short-time scattering, consider for simplicity an initial condition such as that in figure 1 in which $\langle \cos \theta \rangle_0 = 1$. Then if $\alpha t \ll 1$ it follows from (4.3) that

$$\langle \theta^2 \rangle \approx 2\alpha t. \quad (4.4)$$

To test our analytic result for the diffusivity α , we numerically integrate the ray-tracing equations (2.2) for surface waves with initial period of 10s propagating through an ensemble of stochastic velocity fields created by assigning random phases to each Fourier component of the stream function ψ and velocity potential ϕ .

The energy spectrum of the sea surface velocity is modelled with power laws $\tilde{E}^\psi(q)$ and $\tilde{E}^\phi(q) \propto q^{-n}$, with $q_1 < q < q_2$ and no energy outside the interval (q_1, q_2) . The spectra are normalized with prescribed mean square velocities \mathcal{U}_ψ^2 and \mathcal{U}_ϕ^2 as in (3.19). For $n \neq 2$ the integral in (3.20) is evaluated as:

$$\alpha = \frac{2}{c} \frac{(n-1)}{(n-2)} \frac{(q_1^{2-n} - q_2^{2-n})}{(q_1^{1-n} - q_2^{1-n})} \mathcal{U}_\psi^2, \quad (4.5)$$

whereas for $n = 2$

$$\alpha = \frac{2}{c} \frac{q_1 q_2}{q_2 - q_1} \ln \left(\frac{q_2}{q_1} \right) \mathcal{U}_\psi^2. \quad (4.6)$$

We take $q_1 = 2\pi/150\text{km}$ and $q_2 = 2\pi/1\text{km}$ and spectral slopes $n = (5/3, 2.0, 2.5, 3.0)$. For each n we consider three cases corresponding to the three columns in figure 1:

- $\mathcal{U}_\psi = 0.1\text{m s}^{-1}$ and $\mathcal{U}_\phi = 0$;
- ◇ $\mathcal{U}_\psi = 0$ and $\mathcal{U}_\phi = 0.1\text{m s}^{-1}$;
- + $\mathcal{U}_\psi = 0.1\text{m s}^{-1}$ and $\mathcal{U}_\phi = 0.1\text{m s}^{-1}$.

Figure 2 summarizes the results by showing $\langle \theta^2 \rangle$ as a function of time obtained by averaging 2000 rays. The results are in agreement with (4.4) using α obtained from (4.5) and (4.6). In particular there is good agreement between $\langle \theta^2 \rangle$ for case ○ and the analytic result (solid lines). As expected, the potential component of the velocity has no effect on the diffusion of wave action. Thus in case ◇ — pure potential flow — there is no diffusion of action. In case + the flow has twice as much kinetic energy (and shear) as in cases ○ and ◇. But doubling the strength of the flow, by adding a ϕ component, does not significantly increase action diffusion above that of case ○.

We also verified that Monte Carlo results are in agreement with (4.3) when $\alpha t \sim 1$ (not shown).

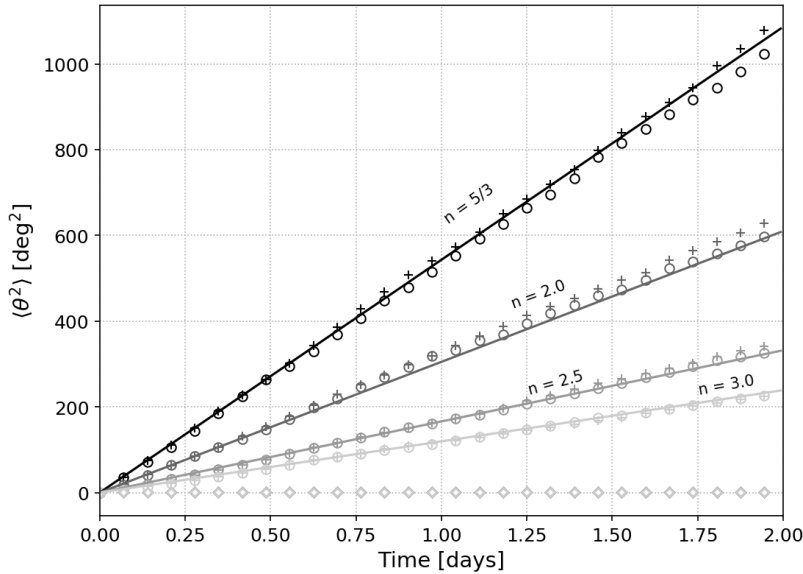


FIGURE 2. Comparison between the ray tracing ensemble average (markers) and the analytical solution (solid lines). Here we show the results for an energy spectrum with spectral slopes following a q^{-n} power-law where $n = 5/3, 2, 2.5$, or 3 . Circles \circ are the result for solenoidal flows; diamonds \diamond , for potential flows; and crosses $+$ for the combination of solenoidal and potential. The solenoidal and potential flows have mean square velocity $0.01 \text{ m}^2/\text{s}^2$, whereas the combined flow $+$ has mean square velocity $0.02 \text{ m}^2/\text{s}^2$. The initial period and direction of the waves are 10s and 0° , respectively.

5. Conclusions

Our expression for the action diffusivity in (2.6) assumes that the WKB approximation is valid and that $U/c \ll 1$. Typical sea-surface currents are of order 0.1 m s^{-1} while the swell band has group velocities that exceed 5 m s^{-1} . Thus $U/c \ll 1$ is not restrictive. Our analysis also neglects effects associated with vertical shear of the flow, which would modify the Doppler-shifted dispersion relationship (Kirby & Chen 1989).

We derived an expression for the diffusivity of surface wave action in (2.6) and demonstrated that for isotropic surface currents the action diffusivity can be expressed in terms of the kinetic energy spectrum of the flow as in (3.20). This result shows that the potential component makes no contribution to action diffusion. Our results are illustrated both qualitatively (figure 1) and quantitatively (figure 2) by numerical solution of the ray equations. Although the numerical examples presented here were obtained for synthetic flows having random phase, the results are also valid in the presence of coherent structures, such as axisymmetric vortices, as long as the statistics remain isotropic (not shown). To leading order, there is no difference between the diffusivity obtained for rays propagating through a pure solenoidal flow and the same solenoidal flow with the addition of an equally strong potential component. In other words, provided that $U/c \ll 1$, the horizontally divergent and irrotational component of the sea-surface velocity has no effect on the action diffusion of surface gravity waves.

Recent studies motivated by the upcoming Surface Water and Ocean Topography (SWOT) satellite mission have found that surface kinetic energy spectra in the ocean are marked by a transition scale from balanced geostrophic motions (horizontally non-divergent) to unbalanced horizontally divergent motions such as inertia-gravity waves (e.g., Qiu *et al.* 2018; Morrow *et al.* 2019). At scales shorter than this “transition” scale,

the kinetic energy spectrum of the potential component of the currents has been observed to dominate over the solenoidal component. In this regime, only a small fraction of the total kinetic energy of the flow would be contributing to the diffusion of surface wave action.

Perhaps the most important application of our results is in the realm of operational surface wave models. Wave models, such as WaveWatch III, solve the action balance equation (2.3) with additional terms to account for wind forcing, non-linear interactions, and wave dissipation (WAVEWATCH III Development Group 2009). Explicitly solving for wave-current interactions in surface-wave models poses two main challenges: it is computationally costly and surface current observations at scales shorter than 100 km are rare (Ardhuin *et al.* 2012). The wave action diffusivity calculated here can be easily implemented as an additional term in operational wave models allowing the effects of the currents to be accounted for based on statistical properties of the sea-surface velocity.

Declaration of Interests. The authors report no conflict of interest.

Acknowledgements

The authors thank Bruce D. Cornuelle, Sarah T. Gille, Matthew R. Mazloff and Jacques Vanneste for helpful discussion and suggestions and Guilherme Castelão for helping with the optimization of the ray-tracing solver. ABVB was funded by NASA Earth and Space Science Fellowship award number 80NSSC17K0326. WRY is supported by the National Science Foundation Award OCE-1657041.

Appendix A. The induced diffusion approximation

In this appendix we reprise the KSV multiscale derivation of the induced diffusion approximation showing that the KSV assumption that \mathbf{U} is incompressible is not necessary. All that is required is spatial homogeneity of the statistical properties of the sea-surface velocity \mathbf{U} .

We follow KSV and introduce a parameter $\epsilon \stackrel{\text{def}}{=} |\mathbf{U}|/c \ll 1$ into the conservation equation of wave action (2.3) by writing $U_m \mapsto \epsilon U_m$. With slow space and time scales $\mathbf{X} = \epsilon^2 \mathbf{x}$ and $T = \epsilon^2 t$, the action equation (2.3) becomes

$$\partial_t A + c_n \partial_{x_n} A + \epsilon^2 \partial_T A + \epsilon^2 c_n \partial_{X_n} A + \epsilon U_n \partial_{x_n} A + \epsilon^3 U_n \partial_{X_n} A - \epsilon k_m U_{m,n} \partial_{k_n} A = 0. \quad (\text{A } 1)$$

With the expansion $A = A_0(\mathbf{X}, \mathbf{k}, T) + \epsilon A_1(\mathbf{x}, \mathbf{X}, \mathbf{k}, t, T) + \dots$ we satisfy the leading-order equation. Then at $\mathcal{O}(\epsilon^1)$:

$$\partial_t A_1 + c_n \partial_{x_n} A_1 = k_m U_{m,n} \partial_{k_n} A_0, \quad (\text{A } 2)$$

with solution

$$A_1 = k_m \int_0^t U_{m,n}(\mathbf{x} - \tau \mathbf{c}) d\tau \partial_{k_n} A_0. \quad (\text{A } 3)$$

At order ϵ^2 the problem is

$$\partial_t A_2 + c_n \partial_{x_n} A_2 + \partial_T A_0 + c_n \partial_{X_n} A_0 = k_i U_{i,j}(\mathbf{x}) \partial_{k_j} A_1 - U_i(\mathbf{x}) \partial_{x_i} A_1. \quad (\text{A } 4)$$

Pulling out ∂_{k_j} from the first term on the right of (A 4) and recombining we obtain

$$\partial_t A_2 + c_n \partial_{x_n} A_2 + \partial_T A_0 + c_n \partial_{X_n} A_0 = \partial_{k_j} k_i U_{i,j}(\mathbf{x}) A_1 - \partial_{x_i} (U_i(\mathbf{x}) A_1). \quad (\text{A } 5)$$

None of these manipulations require $U_{i,i} = 0$. Assuming spatial homogeneity and taking

the average over an ensemble of velocity fields, here denoted by an overbar, the last term on the right of (A 5) is the fast- x derivative of an average, which is zero. In the limit of $t \rightarrow \infty$, and using the expression for A_1 in (A 3), we find

$$\partial_T \bar{A} + c_n \partial_{X_n} \bar{A} = \partial_{k_j} D_{jn} \partial_{k_n} \bar{A}. \quad (\text{A } 6)$$

where \bar{A} is the average of A_0 , defined as an average over an ensemble of velocity fields and

$$D_{jn}(\mathbf{k}) = k_i k_m \int_0^\infty \langle U_{i,j}(\mathbf{x}) U_{m,n}(\mathbf{x} - \tau \mathbf{c}) \rangle d\tau. \quad (\text{A } 7)$$

We now write $U_i(\mathbf{x})$ and $U_m(\mathbf{x} - \tau \mathbf{c})$ in terms of inverse Fourier transforms, such as

$$U_i(\mathbf{x}) = \int e^{i\mathbf{q} \cdot \mathbf{x}} \tilde{U}_i(\mathbf{q}) \frac{d\mathbf{q}}{(2\pi)^2}. \quad (\text{A } 8)$$

After substituting these representations into (A 7), calculations involving the identity

$$\langle \tilde{U}_i(\mathbf{q}) \tilde{U}_m(\mathbf{q}') \rangle = (2\pi)^2 \delta(\mathbf{q} + \mathbf{q}') \tilde{V}_{im}(\mathbf{q}) \quad (\text{A } 9)$$

show that

$$\langle U_{i,j}(\mathbf{x}) U_{m,n}(\mathbf{x} - \tau \mathbf{c}) \rangle = e^{i\mathbf{q} \cdot \tau \mathbf{c}} \int q_j q_n \tilde{V}_{im}(\mathbf{q}) \frac{d\mathbf{q}}{(2\pi)^2}, \quad (\text{A } 10)$$

where $\tilde{V}_{im}(\mathbf{q})$ is the Fourier transform of $V_{im}(\mathbf{r})$, as in (2.7). Substituting (A 10) into (A 7), switching the order of the integrals, and using

$$\int_0^\infty e^{i\mathbf{q} \cdot \tau \mathbf{c}} d\tau = \pi \delta(\mathbf{q} \cdot \mathbf{c}) = \pi k \delta(\mathbf{q} \cdot \mathbf{k})/c, \quad (\text{A } 11)$$

we obtain D_{jn} in (2.6). In (A 11) we have parted company with KSV by taking advantage of the isotropic dispersion relation of surface gravity waves — that is $\mathbf{c} = c\mathbf{k}/k$ — to simplify $\delta(\mathbf{q} \cdot \mathbf{c})$.

REFERENCES

- ARDHUIN, F, GILLE, ST, MENEMENLIS, D, ROCHA, CB, RASCLE, N, CHAPRON, B, GULA, J & MOLEMAKER, J 2017 Small-scale open ocean currents have large effects on wind wave heights. *J. Geophys. Res: Oceans* **122** (6), 4500–4517.
- ARDHUIN, F, ROLAND, A, DUMAS, F, BENNIS, A-C, SENTCHEV, A, FORGET, P, WOLF, J, GIRARD, F, OSUNA, P & BENOIT, M 2012 Numerical wave modeling in conditions with strong currents: Dissipation, refraction, and relative wind. *J. Phys. Oceanogr.* **42** (12), 2101–2120.
- BÜHLER, O, CALLIES, J & FERRARI, R 2014 Wave–vortex decomposition of one-dimensional ship-track data. *J. Fluid Mech.* **756**, 1007–1026.
- CAVALERI, L, FOX-KEMPER, B & HEMER, M 2012 Wind waves in the coupled climate system. *Bulletin of the American Meteorological Society* **93** (11), 1651–1661.
- D’ASARO, EA & OTHERS 2018 Ocean convergence and the dispersion of flotsam. *Proc. Nat. Acad. Sci.* **115** (6), 1162–1167.
- DYSTHE, KB 2001 Refraction of gravity waves by weak current gradients. *J. Fluid Mech.* **442**, 157–159.
- GALLET, B & YOUNG, WR 2014 Refraction of swell by surface currents. *J. Mar. Res.* **72** (2), 105–126.
- HELLER, EJ, KAPLAN, L & DAHLEN, A 2008 Refraction of a Gaussian seaway. *J. Geophys. Res.: Oceans* **113** (C9).
- HENDERSON, SM, GUZA, RT, ELGAR, S & HERBERS, THC 2006 Refraction of surface gravity waves by shear waves. *J. Phys. Oceanogr.* **36** (4), 629–635.

- KAFIABAD, HA, SAVVA, MAC & VANNESTE, J 2019 Diffusion of inertia-gravity waves by geostrophic turbulence. *J. Fluid Mech.* **869**, R7.
- KENYON, KE 1971 Wave refraction in ocean currents. *Deep-Sea Res. and Oceanographic Abstracts* **18** (10), 1023–1034.
- KIRBY, JT & CHEN, T-M 1989 Surface waves on vertically sheared flows: approximate dispersion relations. *J. Geophys. Res: Oceans* **94** (C1), 1013–1027.
- LANDAU, LD & LIFSHITZ, EM 1987 Fluid Mechanics.
- MCCOMAS, CH & BRETHERTON, FP 1977 Resonant interaction of oceanic internal waves. *J. Geophys. Res.* **82** (9), 1397–1412.
- MEI, CC 1989 *The Applied Dynamics of Ocean Surface Waves*, , vol. 1. World Scientific.
- MORROW, R & OTHERS 2019 Global observations of fine-scale ocean surface topography with the surface water and ocean topography (SWOT) mission. *Frontiers in Marine Science* **6**, 232.
- PEREGRINE, DH 1976 Interaction of water waves and currents. In *Advances in Applied Mechanics.*, , vol. 16, pp. 9–117. Elsevier.
- PHILLIPS, OM 1966 *The Dynamics of the Upper Ocean*. Cambridge University Press.
- QIU, B, CHEN, S, KLEIN, P, WANG, J, TORRES, H, FU, L.-L. & MENEMENLIS, D 2018 Seasonality in transition scale from balanced to unbalanced motions in the world ocean. *J. Phys. Oceanogr.* **48** (3), 591–605.
- QUILFEN, Y & CHAPRON, B 2019 Ocean surface wave-current signatures from satellite altimeter measurements. *Geophys. Res. Lett.* **46** (1), 253–261.
- QUILFEN, Y, YUROVSKAYA, M, CHAPRON, B & ARDHUIN, F 2018 Storm waves focusing and steepening in the Agulhas current: Satellite observations and modeling. *Remote Sensing of Environment* **216**, 561–571.
- ROCHA, CB, CHERESKIN, TK, GILLE, ST & MENEMENLIS, D 2016 Mesoscale to submesoscale wavenumber spectra in Drake Passage. *J. Phys. Oceanogr.* **46** (2), 601–620.
- VILLAS BÔAS, AB & OTHERS 2019 Integrated observations of global surface winds, currents, and waves: Requirements and challenges for the next decade. *Frontiers in Marine Science* **6**, 425.
- WAVEWATCH III DEVELOPMENT GROUP 2009 User manual and system documentation of wavewatch iii version 3.14, technical note. *Camp Springs MD: US Department of Commerce, National Oceanographic and Atmospheric Administration, National Weather Service, National Centers for Environmental Predictions* .
- WHITE, BS & FORNBERG, B 1998 On the chance of freak waves at sea. *J. Fluid Mech.* **355**, 113–138.